Population persistence under high mutation rate: from evolutionary rescue to lethal mutagenesis

Yoann Anciaux[1]; Amaury Lambert[3,4], Ophélie Ronce[2]; Lionel Roques[5]; Guillaume Martin[2]

[1] Bioinformatics Research Center (BiRC), Aarhus University, C.F. Møllers Allé 8, 8000 Aarhus Denmark

[2]Institut des Sciences de l'Evolution de Montpellier, Université de Montpellier, CNRS, IRD, EPHE, Montpellier, France

[3]Center for Interdisciplinary Research in Biology (CIRB), Collège de France, CNRS UMR 7241, INSERM U1050, PSL Research University, Paris, France;

[4]Laboratoire de Probabilités, Statistique et Modélisation (LPSM), Sorbonne Université, CNRS UMR 8001, Paris, France

[4] BioSP, INRA, 84914, Avignon, France

Contact Information : yoann.anciaux@birc.au.dk

Keywords :

Evolutionary rescue, Fisher's Geometric Model, Fitness landscape, Lethal mutagenesis, Extinction dynamics, Distribution of extinction times

Authors contributions :

Y.A. O.R. and G.M. initiated the idea for the study. YA, A.L, L.R and G.M derived the mathematical results. Y.A. performed the simulations. Y.A. O.R. and G.M. drafted the paper. All authors critically revised the manuscript, and gave approval of the final version for submission.

Conflict of Interest Statement :

The authors declare no conflict of interests.

Acknowledgments: This work benefited from discussions with S. Gandon, R. Gomulkiewicz, O. Tenaillon and F. Débarre. This work was supported by the French Ministry of Higher Education, Research and Innovation (MESRI allocation doctorale to Y.A.), Agence Nationale de la Recherche (ANR-13-ADAP-0016 "Silentadapt" to G.M. and ANR-13-ADAP-0006 "MeCC" to O.R., ANR-14-CE25-0013 "NONLOCAL" to L.R.) .This is ISEM publication ISEM 2019-XXX.

Data Accessibility Statement :

The authors state that there is no data to be archived.

Abstract

Populations may genetically adapt to severe stress that would otherwise cause their extirpation. Recent theoretical work, combining stochastic demography with Fisher's Geometric Model of adaptation, has shown how evolutionary rescue becomes unlikely beyond some critical intensity of stress. Increasing mutation rates may however allow adaptation to more intense stress, raising concerns about the effectiveness of treatments against pathogens. This previous work assumes that populations are rescued by the rise of a single resistance mutation. However, even in asexual organisms, rescue can also stem from the accumulation of multiple mutations in a single genome. Here, we extend this model to study the rescue process in an asexual population where the mutation rate is sufficiently high so that such events may be common. We predict both the ultimate extinction probability of the population and the distribution of extinction times. We compare the accuracy of different approximations covering a large range of mutation rates. Moderate increase in mutation rates favors evolutionary rescue. However, larger increase leads to extinction by the accumulation of a large mutation load, a process called lethal mutagenesis. We discuss how these results could help design "evolution-proof" anti-pathogen treatments that even highly mutable strains could not overcome.

Introduction

Evolutionary rescue (ER) happens when a population confronted to severe stress avoids extinction by genetic adaptation. Understanding and predicting when and how evolutionary rescue occurs is critical in fields as diverse as conservation biology, invasion biology, emergence of new diseases and the management of resistance to treatment in pests and pathogens (see reviews in Gonzalez *et al.* 2013; Carlson *et al.* 2014; Alexander *et al.* 2014; Bell 2017). In all these situations,

genetic variation, be it present before the onset of stress, or generated *de novo* after, is a key ingredient for evolutionary rescue, as expected theoretically (e.g. Gomulkiewicz and Holt 1995) and observed experimentally (e.g Ramsayer *et al.* 2013). Because mutation affects both standing and *de novo* genetic variation, it comes to no surprise that a number of evolutionary rescue models, combining stochastic evolution and demography, have predicted that higher mutation rates were associated with higher probability of evolutionary rescue (Orr and Unckless 2008, 2014; Martin et al. 2013; Anciaux et al. 2018). Few evolutionary rescue experiments have manipulated the mutation rate to test these predictions (reviewed in Bell 2017). For instance, Couce *et al.* (2015) found that two different mutator strains of bacteria with elevated rates of mutations evolved more than 100-fold resistance to antibiotic concentrations that caused the demise of control strains. Mutator alleles are indeed often found in antibiotic resistant strains causing serious health issues (Eliopoulos and Blázquez 2003), raising concern about pathogens escaping our control by evolving higher mutation rates (for theoretical predictions see Taddei *et al.* 1997; Greenspoon and Mideo 2017).

Yet, most mathematical models of evolutionary rescue assume that the population is rescued from extinction by the spread of a single mutant of large effect (Orr and Unckless 2008, 2014; Martin et al. 2013; Anciaux et al. 2018) and do not describe more polymorphic populations where several mutations of smaller effects can combine to allow population growth (see however the work of Uecker and Hermisson (2016) and Uecker (2017) where sexual reproduction allows to produce such rescue genotypes). The latter situation seems in particular to be common in the evolution of herbicide resistance, especially when the mutational target for resistance is large (Kreiner et al. 2018). Even in asexual organisms, when the mutation rate is high, evolutionary rescue may commonly result from the cumulative effect of multiple mutations accumulating stochastically over time in a given lineage. Such a mutation regime is particularly relevant in highly mutable viruses, mutator strains of bacterial (e.g. Springman *et al.* 2010) or cancer cells (e.g. Loeb 2001). Our aim here is to provide theoretical predictions for evolutionary rescue in such a regime with high mutation rates in asexual organisms, complementing existing theory on the subject.

Several complications arise when modelling evolutionary rescue in highly polymorphic populations with high mutation rates. First, the dynamics of allelic frequencies at different loci

interact in asexuals. For example, the selective sweep of a given beneficial mutation is hindered by the co-segregation of other beneficial mutations (clonal interference, Gerrish and Lenski 1998). A theoretical study by Wilson *et al.* (2017) recently showed that, when evolutionary rescue is likely, it should most often be driven by soft selective sweeps, where multiple resistance mutations spread through the population simultaneously. Wilson *et al.* (2017) still assumed that each of these lineages carried a single mutation, each with the same effect on the population growth rate. When the mutational target is large, different lineages contributing to rescue are however likely to carry mutations with different fitness effects. Modelling the distribution of mutation effects (as in Martin *et al.* 2013; Anciaux *et al.* 2018) becomes then critical. Finally, when the mutation rate is high, multiple mutations may also accumulate on each lineage, either facilitating evolutionary rescue or impeding it, through their *cumulative* effect. Modelling both beneficial and deleterious mutations and, critically, the epistatic interactions between them, also becomes necessary.

Previous evolutionary rescue theory predicts that higher mutation rate allows populations to withstand higher levels of stress (e.g. Anciaux *et al.* 2018). Yet, there are reasons to expect this prediction not to hold above some critical mutation rate. Indeed, increased mutation rates also build-up detrimental mutation loads. Mimicking this mutation load through a constant cost associated with the mutator genotypes, Greenspoon and Mideo (2017) found that the evolution of elevated mutation rates facilitated evolutionary rescue only in a limited range of situations. The variance load, depressing mean fitness despite ongoing adaptation, is a critical component of quantitative genetics models assuming a non-linear relationship between fitness and phenotypes and increases under higher mutation rates (e.g. Bürger and Krall 2004). Artificially increasing the mutation rate has even been proposed as a mean to weaken or even eliminate pathogen populations, by a process denoted lethal mutagenesis (Loeb et al. 1999). Models of lethal mutagenesis predict that extinction of the target population could be observed under biologically realistic sets of parameters (Bull et al. 2007; Martin and Gandon 2010; Wylie and Shakhnovich 2012). In these models, mean fitness dynamics and extinction stem from the deterministic effects of selection and mutation. Alternatively, Matuszewski *et al.* (2017) discuss the continuity between these models and models of mutational meltdown, where extinction is driven by the interaction of genetic drift and deleterious mutation. Lethal mutagenesis has been investigated empirically for

115 treatment against viruses (Springman et al. 2010; Arias et al. 2014), bacteria (Bull and Wilke 2008)
116 or cancer cells (Liu et al. 2015). In particular, the combination of antiviral treatments with
117 mutagenic agents is investigated as a strategy to fight fast evolving viruses, such as influenza (Bank
118 et al. 2016). It seems important to improve our ability to predict whether and when such mutagenic
119 agents will increase treatment efficacy or, conversely, facilitate the evolution of resistance.

120 The population genetics of adaptation behind the rescue process, in isolated asexual
121 populations, sketchily fall into two alternative regimes: rescue may stem (i) from single mutations
122 of large effect (strong selection weak mutation 'SSWM' regime) or (ii) from multiple mutations of
123 small effects (weak selection strong mutation 'WSSM' regime) (reviewed in Alexander *et al.* 2014).
124 The SSWM regime of adaptation has been extensively investigated via "origin-fixation" models
125 describing the average behavior of stochastic evolutionary dynamics (McCandlish and Stoltzfus
126 2014) whereas the WSSM regime has been widely analyzed via deterministic models of
127 quantitative genetics (Lande 1976, 1980). Corresponding evolutionary rescue models further
128 include a coupling of adaptation and demographic dynamics, and naturally fall into the same two
129 regimes (discussed in Anciaux *et al.* 2018). The SSWM regime of evolutionary rescue is
130 characterized by the fact that the first resistant lineage to establish (and thus cause rescue) is only
131 at one mutational step from the dominant sensitive 'wild-type' lineage (e.g. Feder *et al.* 2016).
132 Models that describe highly polymorphic dynamics (WSSM regimes) often use the infinitesimal
133 model assumptions (many unlinked polymorphic loci), which does not apply to asexual
134 populations. In the WSSM regime, the exact stochastic evolutionary dynamics become quickly
135 intractable, and have often been studied by simulation (e.g. Boulding and Hay 2001). The latter
136 models further often consider initial standing genetic variance as given and pay little attention to
137 the effect of mutation rates in maintaining this variance. They often ignore *de novo* mutations after
138 the onset of stress, on the argument of short timescales being most critical for evolutionary rescue
139 (e.g. (Gomulkiewicz et al. 2010)). The dichotomy between SSWM and WSSM entails a somewhat
140 simplistic view of adaptation regimes, at the two extremes of all possible mutation rates. These
141 approximations reflect different views of population genetics, which both have received empirical
142 support.

143 To make analytical progress in our understanding of the effect of mutation rates on the
144 process of evolutionary rescue, we here built on two recent theoretical developments (Martin and
145 Roques 2016; Anciaux et al. 2018). As in Anciaux *et al.* (2018), we study evolutionary rescue using
146 Fisher's (1930) geometric model (hereafter "FGM") to model the distribution of mutation effects
147 on fitness. The FGM (detailed in Methods) is a single peak phenotype-fitness landscape where
148 fitness depends on the position, in phenotype space, of a given genotype relative to an optimum.
149 In the context of ER, stress may affect this landscape in various ways (height, width or position of
150 the peak). In this model, the distribution of mutation effects (both beneficial and deleterious)
151 depend on the context, both genotypic (epistasis) and environmental (e.g. effect of stress). These
152 key features of the FGM are qualitatively and sometimes even quantitatively consistent with a
153 wealth of empirical observations (reviewed in Tenaillon 2014). Under the assumptions of FGM,
154 rescue mutants become very rare as the intensity of stress increases, because they require very
155 large mutational steps. As a consequence, Anciaux *et al.* (2018) predict that there is a narrow
156 window of stress levels where the probability of rescue shifts from being very likely to very unlikely.
157 They also predict that this critical level of stress, beyond which adaptation is unlikely, is increased
158 by higher mutation rates (Anciaux et al. 2018). Yet, predictions of this model apply to the SSWM
159 regime and may not hold for high mutation rates.

160 Here, we extend our previous analysis of evolutionary rescue over Fisher's geometric model
161 (Anciaux et al. 2018) to the more complex and polymorphic WSSM regime. To do so, we use the
162 approach in Martin and Roques (2016) to model the non-equilibrium dynamics of fitness
163 distributions, in large asexual populations with epistasis. In particular, Martin and Roques (2016)
164 showed that, under the FGM, while the fitness dynamics are more complex at higher mutation
165 rates, they are also more predictable and less prone to stochastic fluctuations, even in relatively
166 small populations. To model evolutionary rescue, we still need to describe the demographic
167 stochasticity associated with the extinction process. In the WSSM regime, we thus use a
168 combination of two analytically tractable theories: a deterministic approximation to the dynamics
169 of mean fitness (from Martin and Roques 2016) and a diffusion approximation to the stochastic
170 dynamics of population sizes (from Bansaye and Simatos 2015).

171 Beyond a derivation of the probability of ultimate rescue or extinction, this approach
172 further allows tracking the rescue process over time. As stated in Gomulkiewicz *et al.* (2017),
173 transient dynamics (population size dynamics, distributions of extinction times) are of high interest
174 for applications of evolutionary rescue theory, yet are not available from existing predictions,
175 which focused mainly on ultimate outcomes. Gomulkiewicz *et al.* (2017) studied the distribution
176 of extinction times for populations doomed to extinction, mostly in the absence of mutation (i.e.
177 with a fixed arbitrary set of competing asexual genotypes at the onset of stress). The present work
178 allows extending this analysis to include frequent *de novo* mutation, rescue events involving several
179 mutational steps, epistasis, variable mutation effects depending on stress intensity and an explicit
180 description of the dynamics of mutation load. Our approach captures the continuum from
181 evolutionary rescue to lethal mutagenesis, as mutation rate increases. Interestingly, some
182 parameter ranges prove to greatly limit evolutionary rescue at all mutation rates, i.e. in spite of the
183 possible apparition of mutators.

184

185 ## Methods

186 ### I. General framework

187 The population is initially adapted to a non-stressful environment where its mean growth
188 rate is positive. At the onset of stress, the population size is N_0 and the mean growth rate of the
189 population shifts to a negative value due to the new stressful environment. Without evolution, the
190 population is doomed to extinction. Evolutionary rescue occurs if at least one resistant lineage
191 (with a positive growth rate in the new environment) establishes, in spite of demographic
192 stochasticity. These resistant mutant lineages can either already be present in the population or
193 arise *de novo* after the onset of stress. It is thus crucial to determine how the number and growth
194 rates of such mutants depend on the new environmental conditions and on the parental genotypes
195 already present in the population. We do so using the FGM detailed below.

196

197 *Fitness landscape*

198 In the FGM, a given phenotype is a vector in a phenotypic space of n dimensions that
199 determine fitness (here the growth rate r). The phenotype of an individual with genotype i, is
200 characterized by a vector $\mathbf{z}_i \in \mathbb{R}^n$ of the breeding values (heritable components) for the n traits,
201 and its growth rate is r_i. Formulated this way, the model thus accommodates micro-environmental
202 effects on phenotypes (partial heritability), but not systematic (plastic) shifts in phenotype with
203 stress. In a given environment, fitness decays as a quadratic function of the phenotypic distance to
204 a single phenotypic optimum, where the growth rate r_{max} is maximal at a given absolute level
205 (height of the fitness peak). We assume that each environment is associated with a single optimum
206 and fitness peak. In the scenario investigated here, in the non-stressful environment, the
207 population is close to the 'ancestral' optimum $\mathbf{z}_A$. When the environment changes, it is assumed
208 to determine a new optimum $\mathbf{z}_*$. Without loss of generality, the height of the peak may also differ
209 between the ancestral and new environments. However, we do require that the n dimensions that
210 determine fitness remain the same (in nature and number) across environments. In the new
211 environment, the growth rate of an individual with genotype i is given by:

$$r(\mathbf{z}_i, \mathbf{z}_\star) = r_{max} - \frac{\|\mathbf{z}_i - \mathbf{z}_*\|^2}{2}. \quad [1]$$

212 This is an isotropic version of the FGM (all directions are equivalent for selection and mutation)
213 where phenotypes are scaled by selective strength.

214

215 *Stochastic demographic dynamics*

216 We restrain our analysis to finite haploid asexual populations. Individuals have independent
217 evolutionary and demographic fate (frequency or density dependence are ignored). Each genotype
218 i has a growth rate r_i and a reproductive variance σ_i ($r_i = r(\mathbf{z_i}, \mathbf{z}_*)$ in a given environment with
219 optimum $\mathbf{z}_*$), which define its stochastic demographic parameters in the context of a Feller
220 diffusion approximation (Feller 1951), as in e.g. Martin *et al.* (2013), Gomulkiewicz *et al.* (2017) or
221 Anciaux *et al.* (2018). For simplicity, we further assume here that the average stochastic variance
222 in reproduction is constant over time: $\bar{\sigma}(t) = 1/K_t \sum_{i=1}^{K_t} \sigma_i = \bar{\sigma}$, where the average is taken over

the K_t genotypes present at time t. This can for example be accurate whenever the σ_i are roughly constant across genotypes i (discussed in Martin *et al.* 2013 and Anciaux *et al.* 2018).

Notation	Description	Formula
N_t, N_0	N_t: population size at time t after the onset of the stress. N_0: initial population size at the onset of the stress.	
U	Mutation rate *per* individual *per* unit time.	
n	Number of traits under stabilizing selection, or phenotypic dimensionality.	
λ	Variance of mutational effects: variance of the phenotypic effects of mutations, per trait, in a trait space scaled by the strength of stabilizing selection	$\mathbf{dz} \sim N(\mathbf{0}, \lambda\, \mathbf{I}_n)$
$\mathbf{z}$	n-dimensional vector $\mathbf{z} \in \mathbb{R}^n$ of (breeding values for) phenotype	
$\mathbf{z}_A, \mathbf{z}_*$	$\mathbf{z}_*$: optimal phenotype in the new environment $\mathbf{z}_A$: average phenotype of the ancestral population (before the onset of stress)	
r, σ	Growth rate (r) and reproductive variance (σ) of a given genotype, in the new environment.	Eq.[1]
$\overline{r}_t, \overline{\sigma}$	Mean growth rate ($\overline{r}_t$) and mean reproductive variance ($\overline{\sigma}$) of the population, in the new environment.	Eqs. [2] and [3]
r_{max}	Maximum possible growth rate in the new environment.	$r(\mathbf{z}_*) = r_{max}$
r_D	Rate of decay of the ancestral phenotype $\mathbf{z}_A$ in the new environment.	$r(\mathbf{z}_A) = r_{max} - \lVert \mathbf{z}_A \rVert^2/2 = -r_D$
y_D	Rate of decay scaled by r_{max}.	$y_D = r_D/r_{max}$
ϵ	Ratio between the mutational load and the maximal growth rate	$\epsilon = n\,\mu/(2\, r_{max})$
ω_{DN}, ω_{DN+SV}	ω_{DN}: rate of rescue from *de novo* mutations scaled by N_0 ω_{SV}: rate of rescue from both *de novo* and standing variance scaled by N_0	Eqs.[5],[6]
P_{ext}, P_R	P_{ext} : Extinction probability P_R : Rescue probability	P_{ext} see Eq.[4] $P_R = 1 - P_{ext} = 1 - e^{-N_0\,\omega_R}$
U_c	Critical mutation rate beyond which the WSSM regime is valid.	$U_C = n^2\,\lambda/4$
U_{max}	Mutation rate beyond which certain extinction is enforced by lethal mutagenesis	$U_{max} = 4\, r_{max}^2/(n^2\,\lambda)$
U_*	Mutation rate at which the rescue probability rises to 1/2	Eq.[7]
$r_D^*(p)$	Rate of decay for which the maximal rescue probability for any U or λ is equal to p	Eq.[8]

***Table 1**: Notations*

II. Evolutionary dynamics.

In this section, we describe the model of evolutionary dynamics over the fitness landscape (FGM of the previous section), which is embedded into the ER model. In the following, *de novo* mutations (appearing after the onset of stress) are denoted "DN" and mutations from standing genetic variation (mutants already present before the onset of stress) are denoted "SV". Correspondingly, evolutionary rescue dynamics from an isogenic population, adapting only from *de novo* mutations, are labelled "DN" and dynamics from a polymorphic population, adapting from both *de novo* mutations and standing genetic variation, are labelled "$\mathrm{DN} + \mathrm{SV}$".

1. Evolutionary dynamics from an isogenic population.

The population is maladapted in the new stressful environment and its growth rate is $-r_D$, corresponding to a decay rate $r_D > 0$. Mutations arise every generation following a Poisson process with rate U per unit time per capita. For a given parent phenotype, each mutation creates a random perturbation $\boldsymbol{dz}$ on phenotype, which is unbiased and follows an isotropic multivariate Gaussian distribution, $\boldsymbol{dz} \sim \mathcal{N}(0, \lambda\, \mathbf{I}_n)$ where $\mathbf{I}_n$ is the identity matrix in n dimensions and λ is the variance of mutational effects on traits, standardized by the strength of selection. Mutation effects add-up on phenotype, but not on fitness because $r(.)$ is nonlinear (epistasis on fitness and not on phenotype).

In the WSSM regime, the mean growth rate of the population shows limited stochastic variation among replicates, even in reasonably small populations. We thus approximate the evolutionary process by a deterministic fitness trajectory, derived in the WSSM regime under the FGM (Martin and Roques 2016). This seemingly rough approximation can be justified *a priori*: most of the ER process is determined by the speed at which the population adapts at the very onset of stress. This early trajectory takes place when the population is still large and the adaptive process proves to be relatively deterministic, especially over this short timescale, provided that the mutation rate is high enough (WSSM: $U \gg U_c = n^2\lambda/4$). Both analytical arguments and simulations, detailed in (Martin and Roques 2016), showed that mean fitness trajectories are

256 indeed close to the deterministic prediction (with limited variation among replicates), provided
257 that $U \gg U_c$ (WSSM) and $NU \gg 1$ (large mutational input). Here, we use the deterministic fitness
258 trajectory corresponding to these conditions to approximate the growth rate trajectory of all
259 replicate populations under stress.

260 Provided $U \gg U_c$ we thus approximate the trajectory of the mean growth rate of all replicate
261 populations by its deterministic trajectory for the WSSM (Martin and Roques 2016):

$$\bar{r}_t^{\mathrm{DN}} \approx r_{max} - (r_D + r_{max})\,\mathrm{sech}(\mu\, t)^2 - \frac{n}{2}\,\mu\,\tanh(\mu\, t), \qquad [2]$$

262 where $\mathrm{sech}(z) = 2/(e^z + e^{-z})$ is the hyperbolic secant, $\tanh(z) = (e^z - e^{-z})/(e^z + e^{-z})$ is the
263 hyperbolic tangent and $\mu = \sqrt{U\lambda}$ is a composite parameter of the mutational parameters. Recall
264 that r_D is the decay rate of the isogenic population and r_{max} is the maximum fitness that can be
265 reached in the new environment (with $r_D + r_{max}$ the fitness distance between the parent
266 genotype's fitness and the top of the fitness peak). The mean growth rate in Eq.[2] reaches a
267 plateau at infinite time of $r_{max} - n\,\mu/2$ corresponding to the maximal growth rate minus the
268 mutational load.

269

270 *2. Evolutionary dynamics from an initially polymorphic population (at mutation-selection balance)*

271 The evolutionary dynamics of rescue from a polymorphic population is obtained by a similar
272 approximation. We assume that the population is initially at mutation-selection balance in the non-
273 stressful environment, with an arbitrary positive mean growth rate. The phenotypic distribution at
274 the onset of stress is centered on a mean phenotype $\bar{\mathbf{z}}$, which growth rate in the new environment
275 is used to characterize the harshness of the stress imposed. For consistency with the isogenic
276 population model above, we thus denote this growth rate $-r_D = r(\bar{\mathbf{z}}, \mathbf{z}_*)$, where $r_D > 0$ is the
277 decay rate of the central genotype as in the previous section. Resistant genotypes may already be
278 present in the population at the onset of stress ("SV") or appear by *de novo* mutation ("DN"), or
279 arise as combinations of these (multiple step rescue mutants). Using the same reasoning as in the

280 previous subsection, we approximate the mean growth rate of all replicate populations by the
281 deterministic trajectory for the WSSM, i.e. whenever $U \gg U_c$ (Martin and Roques 2016):

$$\bar{r}_t^{DN+SV} \approx r_{max} - e^{-2\,\mu\,t}(r_D + r_{max}) - \frac{n\,\mu}{2}. \qquad [3]$$

282 In a polymorphic population at mutation-selection balance, the presence of a mutational load
283 implies that the mean growth rate of the population in Eq.[3] is lower than the mean growth rate
284 of an isogenic population in the same environmental conditions, with the same central genotype
285 ($\bar{r}_0^{DN+SV} = r_D - n\,\mu/2$). As in Eq.[2], the mean growth rate in Eq.[3] reaches a plateau at infinite
286 time of $r_{max} - n\,\mu/2$ corresponding to the maximal growth rate minus the mutational load.

287

288 III. Evolutionary rescue probability

289 The demographic dynamics of the whole population can be approximated by an
290 inhomogeneous Feller diffusion (see Appendix I section I) with parameters $\bar{r}_t$ (the mean growth
291 rate) and $\bar{\sigma}$ (the reproductive variance averaged across segregating genotypes): $\bar{r}_t$ may vary
292 stochastically as genotype frequencies change under the effects of drift, selection and mutation.
293 However, as explained in the previous subsection, we approximate each replicate's fitness
294 trajectory by its deterministic expectation under the WSSM regime: $\bar{r}_t \approx \bar{r}_t^{DN}$ or $\bar{r}_t^{DN+SV}$, using the
295 relevant cases from Eqs.[2] or [3]. Therefore, the model approximately reduces to a Feller diffusion
296 with constant $\bar{\sigma}$ and time-inhomogeneous deterministic growth rate $\bar{r}_t$. Under these hypotheses,
297 the demographic dynamics follow the stochastic differential equation: $dN_t = \bar{r}_t\,N_t\,dt +$
298 $\sqrt{\bar{\sigma}\,N_t}\,dB_t$ where B_t is a Weiner process (see Appendix I section I for more details). We can then
299 use the results from Theorem 1 of Appendix II (see also Bansaye and Simatos 2015) on
300 inhomogeneous Feller diffusions to derive the probability that the population is extinct before
301 time t:

$$P_{\text{ext}}(t) = \exp\left(-\frac{2\,N_0}{\bar{\sigma}\,\int_0^t e^{-\rho_u}\,du}\right),$$
$$\rho_u = \int_0^u \bar{r}_v\,dv\ , \qquad [4]$$

where $\bar{r}_t$ is given by Eqs.[2] or [3]. This expression can be evaluated numerically at any time $t > 0$. ER happens whenever evolution (change in $\bar{r}_t$) allows to avoid extinction. Hence, the general form of the rescue probability is readily obtained as the complementary probability of the infinite time limit of Eq.[4], namely the probability of never getting extinct: $P_R = 1 - P_E$ with $P_E = P_{\text{ext}}(\infty)$, the extinction probability after infinite time. Depending on the scenarios, this rescue probability can be computed explicitly, or approximated via Laplace approximations to the integral $\int_0^\infty e^{-\rho_u}\,du$, in some parameter ranges (see Results and Appendix I).

IV. Individual-based stochastic simulations: The analytical predictions are tested against exact stochastic simulations of the population size and genetic composition of populations across discrete, non-overlapping generations. The simulation algorithm is described in Anciaux *et al.* (2018). Briefly, reproduction is Poisson distributed every generations with parameter e^{r_i} for genotype i, mutations occur according to a Poisson process with constant rate U per capita per generation. The phenotypic effects of the mutations are drawn from a multivariate normal distribution, with multiple mutations having additive effects on phenotype. Fitnesses are computed according to the FGM using Eq.[1]. With such a Poisson offspring distribution, the reproductive variance of genotype i is $\sigma_i = 1 + r_i \approx 1$, assuming small growth rates $r_i \ll 1$, in per-generation time units. So this particular demographic model satisfies our assumption of constant $\bar{\sigma}$ in spite of changes in the genotypic composition of the population: here $\bar{\sigma} = 1/K_t \sum_{i=1}^{K_t} \sigma_i \approx 1$. Note also that the analytical derivations (relying on a Feller diffusion (1951) approximation) approximately cover other demographic models (e.g. birth death models, see Martin et al. 2013; Gomulkiewicz et al. 2017), as long as they also satisfy $\bar{\sigma}(t) \approx \bar{\sigma}$ constant.

Results

Rescue probability: general form. In spite of their difference in the population genetics underlying ER, the two scenarios with or without standing variance yield similar expressions for the probability of ER (as shown in Eqs.(A5) and (A11-A12) in Appendix I):

$$P_R = 1 - e^{-N_0\,\omega} \quad \text{with} \quad \omega = \frac{2\,\mu}{\int_0^\infty h(\tau)^{n/2} \exp\big(-\ n/(2\,\epsilon)\ f(\tau)\big)\ d\tau}$$

$$\text{and} \begin{cases} DN: \ f(\tau) = \tau - (1 + y_D)\tanh(\tau)\ ,\ \ h(\tau) = \cosh(\tau) \\ DN + SV: \ f(\tau) = \tau - \dfrac{1}{2}(1 + y_D)(1 - e^{-2\,\tau})\ ,\ \ h(\tau) = e^{\tau} \end{cases}, \qquad [5]$$

where the particular form of the functions $f(.)$ and $h(.)$ depend on the chosen scenario. Here, $\cosh(z) = (e^z + e^{-z})/2$ is the hyperbolic cosinus and we introduce two scaled parameters: $\epsilon = n\,\mu/(2\,r_{max})$ and $y_D = r_D/r_{max}$ (recall that $\mu = \sqrt{U\lambda}$ depends on both mutation rate and effect). The parameter y_D describes how fast the initial clone decays, compared to how fast the optimal genotype grows, it gives a scaled measure of the harshness of the stress imposed (see also Anciaux *et al.* 2018). The parameter ϵ is the ratio of the mutation load (at mutation-selection balance) and the maximal absolute growth rate that can be reached in the stress. Certain extinction by lethal mutagenesis occurs whenever the load is equal or larger than the maximal growth rate (i.e. $\epsilon \geq 1$). A small value of ϵ means that we are far from this certain extinction regime.

The quantity ω in Eq.[5] is akin to a 'per lineage rate of rescue'. Analytical expressions for this rate are either unavailable (DN) or complicated ($DN + SV$, Eq.(A12) in Appendix I).

Weak selection, intermediate mutation approximation: To get a more direct insight into the impact of each parameter, we sought an approximate expression for ω, detailed in Appendix I section III and IV. This approximation applies with an intermediate mutation rate, where ER mainly depends on the early adaptation of the population to stress, and not on the ultimate mutation load (lethal mutagenesis). More precisely, it requires that the WSSM approximation be accurate while ϵ

remains small, which implies a small λ and intermediate U: $n^2\,\lambda/4 \ll U \ll r_{max}$. This is why we call this limit a 'weak selection, intermediate mutation' approximation.

Under this approximation, the *per capita* rate of rescue ω takes a roughly similar form for both scenarios with or without standing variance (detailed in Eqs.(A8) through (A14) in Appendix I):

$$\omega \underset{\epsilon \ll 1}{\approx} 2\sqrt{\frac{r_{max}\,\mu}{\pi}}\,\exp\left(-\frac{r_{max}}{\mu}\,g(y_D)\right)$$
$$\text{with}\begin{cases} DN:\ g(y) = g_{DN}(y) = \sqrt{y(1+y)} - \cosh^{-1}\left(\sqrt{1+y}\right) \\ DN+SV:\ g(y) = g_{DN+SV}(y) = (y - \log(1+y))/2 \end{cases} \qquad [6]$$

In both cases, the function $g(.)$ is positive and increases (roughly log-log linearly) with $y_D = r_D/r_{max}$. The accuracy of this approximation is illustrated in **Supplementary Figures 2** and **3** and **Figures 1** and **2**. Note that, whenever the approximation applies, the ER probability is independent of dimensionality (n).

Sharp decay in ER probability with increasing stress levels: A possible measure of stress intensity in ER is the rate of decay r_D of a population after the environmental change (see also Anciaux *et al.* 2018). However, stress might also affect other parameters of the FGM: the height of the fitness peak r_{max}, the mutation rate U or the variance of mutational effects: λ. We detail the two latter effects (which affect ER via the composite parameter $\mu = \sqrt{U\,\lambda}$), in the next section, and focus here on r_{max} and r_D. As in Anciaux *et al.* (2018), increased r_D means both a faster decay (purely demographic effect of stress) and a larger shift in optimum (which affects the whole distribution of fitness effect of mutations), which both decrease the ER probability. On the contrary, increasing r_{max} increases the ER probability through two effects. First, the size of the phenotypic space of resistance increases with r_{max} (as in the SSWM regime, see Anciaux *et al.* 2018). Second a large r_{max} counterbalances a high mutational load $n\,\mu/2$ as can be seen in Eq.[2] (this latter effect is only captured in the WSSM approximation).

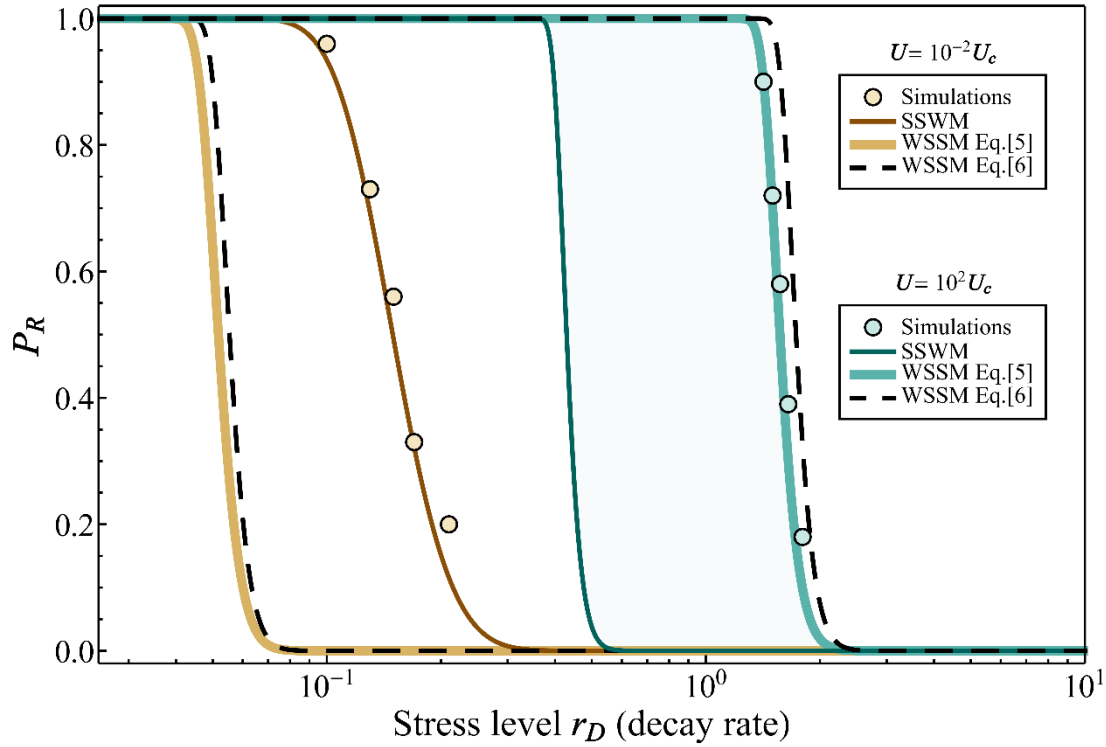

Figure 1*: ER probability against decay rate r_D for a population without standing variance (DN). Dots show the results of 10^2 simulations; thin plain lines: the SSWM approximation (Eq.[6] from Anciaux et al. 2018); thick plain lines: the WSSM approximation in Eq.[5]; dashed lines: the corresponding closed form expression in Eq.[6]. The shaded area corresponds to the extra contribution to ER from multiple mutants, compared to single mutants. All models and simulations are shown for a high mutation rate (blue) or a low mutation rate (brown), indicated in legend. Other parameters are $N_0 = 10^5$, $n = 4$, $r_{max} = 1$ and $\lambda = 5.10^{-3}$.*

Figure 1 illustrates how the ER probability drops sharply with the decay rate r_D, both in the SSWM regime (brown curves, $U \ll U_c$, see legend) and in the WSSM regime (blue curves, $U \gg U_c$). This qualitatively similar behavior is *a priori* due to common geometric constraints imposed by the FGM. The alternative approximations (SSWM *versus* WSSM) capture a different and complementary portion of the range of possible mutation rates: compare the blue ($U = 10^2 U_c$) *vs*. brown ($U = 10^{-2} U_c$) curves and dots in **Figure 1**. Higher mutation rates allow withstanding higher stress levels (large r_D), but it is not their only effect, as we now detail.

385 **Non-monotonous relationship between ER probability and mutational parameters:** In the following
386 section, we now investigate the effect of mutational parameters. Both the mutation rate U and
387 the variance of mutational effects λ affect the system in a similar fashion through the composite
388 parameter $\mu = \sqrt{U\lambda}$. At small t (in Eq.[4]), an increase in μ speeds-up the early adaptive process,
389 thus favoring rescue but also increases the ultimate mutation load, favoring extinction by lethal
390 mutagenesis. These antagonistic effects of μ create a non-monotonic relationship between the
391 rescue probability and mutational parameters. This is illustrated in **Figure 2**, which also shows how
392 Eq.[5] (thick lines) captures this effect, through the parameter $\epsilon = n\,\mu/(2\,r_{max})$). For low stress
393 r_D, P_R is maximal and approximately equal to 1 over a range of mutation rates (plateau **Figure 2**,
394 see also **Supplementary Figure 6** for higher stress values). Beyond this range, the rescue probability
395 in Eq.[5] drops to 0 at $U = U_{max} \equiv (4\,r_{max}^2)/(n^2\,\lambda)$. U_{max} is the mutation rate beyond which
396 certain extinction is enforced by lethal mutagenesis because the mutation load ($\mu\,n/2$) is larger
397 than the maximal growth rate that can be reached in the stress (r_{max}). Hence, even if ER allowed
398 the population to invade the new environment, it could not generate a stable population once at
399 mutation-selection balance.

400 Note that Eq.[6], which is only valid for intermediate μ, does not capture the decrease in P_R close
401 to $U = U_{max}$. It does however capture the increase in P_R as mutation rate increases, far
402 below U_{max}.

403

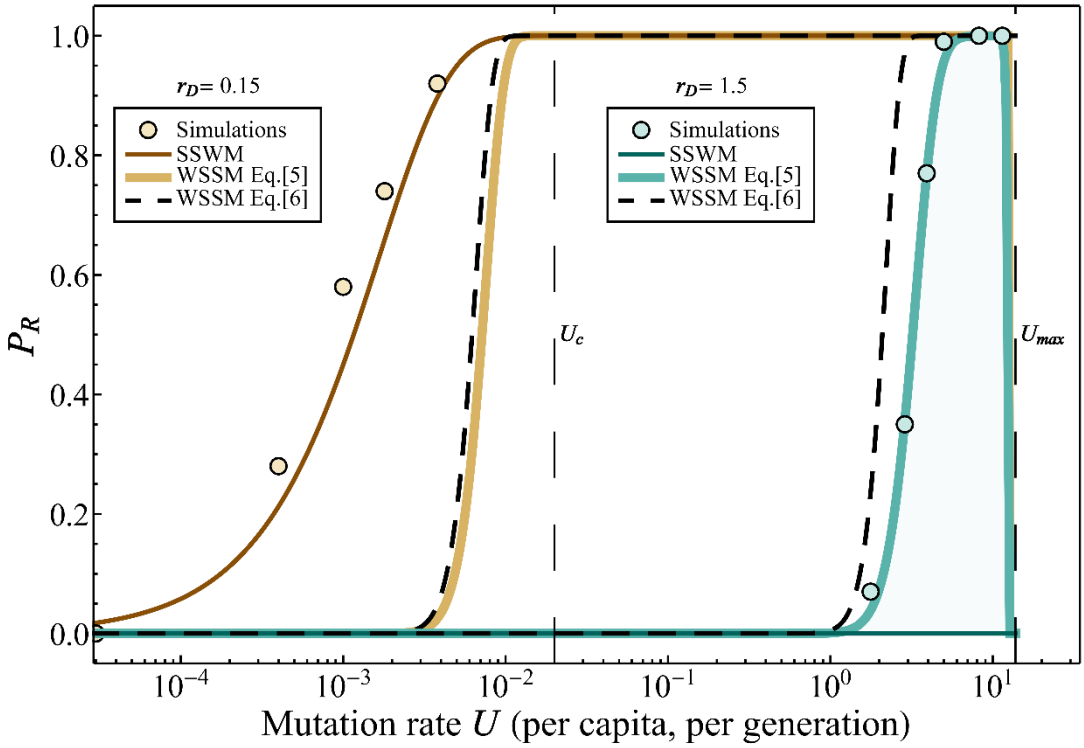

Figure 2: *ER probability against mutation rate U for a population without standing variance (DN). Same legend as* ***Figure 1****. All models and simulations are shown for a high decay rate (blue) or a low decay rate (brown), indicated in legend. Other parameters are $N_0 = 10^5$, $n = 4$, $r_{max} = 0.5$ and $\lambda = 5.10^{-3}$.*

Evolutionary dynamics from an initially polymorphic population (at mutation-selection balance): The results presented in the previous figures illustrate rescue from *de novo* mutations. In the presence of additional standing genetic variation, rescue mutants can arise from *de novo* mutants, from pre-existing genotypes or from a combination of both. **Figure 3** shows the qualitative similarity between the case with and without standing genetic variation, in their dependence on r_D and U, as observed in simulations and captured by Eqs.[5] and [6]. Indeed, **Figure 3** confirms that the addition of standing genetic variation does not qualitatively modify the relationship between the rescue probability and stress intensity (r_D, **Figure 3a**) or mutational parameters (here U, **Figure 3b**). Note that the accuracy of Eq.[5] is lower for higher r_{max}, where the continuous time approximations become less accurate to capture discrete time simulations (see **Supplementary Figure 4**). In the next sections, for the sake of clarity and simplicity, we will mainly discuss the scenario of ER from

de novo mutations only, as the qualitative behaviors are similar with an extra contribution from standing variance.

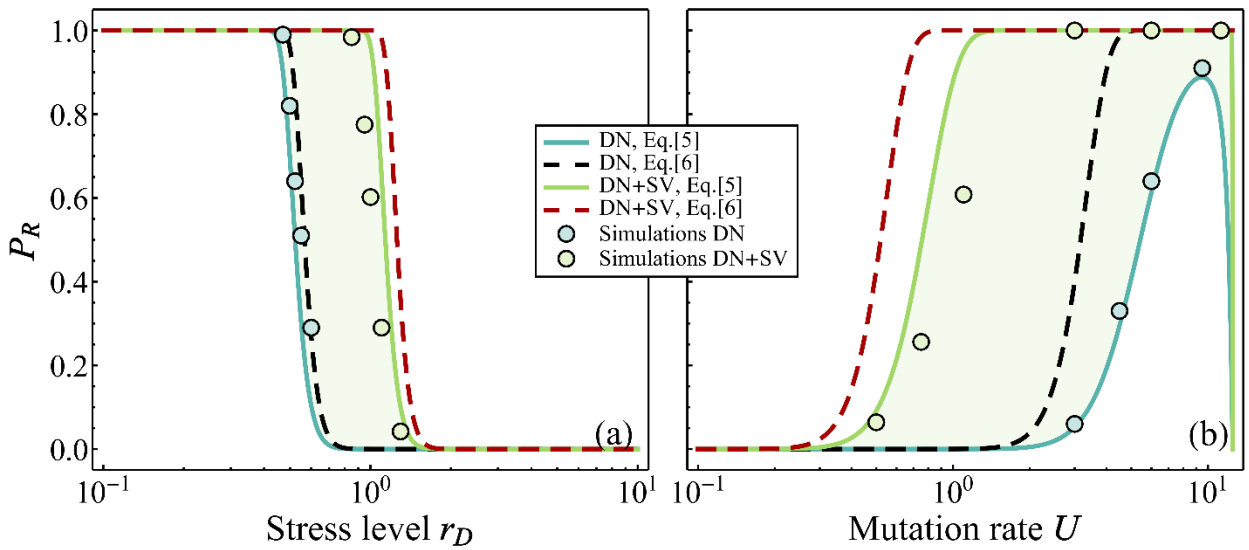

Figure 3*: ER probabilities from de novo mutants only (blue: Eq.[5], black dashed line: Eq.[6]) or from both de novo and pre-existent mutants (green: Eq.[5], red dashed line: Eq.[6]) against the stress level r_D (a) or the mutation rate U (b). Dots show the results of 10^2 simulations (started from 10 simulated populations at mutation-selection balance for the $DN + SV$ scenario). The shaded area corresponds to the contribution from the standing genetic variance to the rescue compared to de novo mutation. Other parameters are $N_0 = 10^5$, $r_{max} = 0.5$, $n = 4$ and $\lambda = 5.10^{-3}$. $U = 10\ U_c$ in panels (a) and $r_D = 1.8$ in panel (b).*

Mutation window for ER: In the previous subsections, we have shown that the ER probability drops sharply with increasing stress and is maximal over a finite range of mutation rates, which we denote "mutation window" for ER. The "width" (range of mutation rates) and "height" (maximum of ER probability over the range) of this window strongly depends on stress.

Width of the window: To characterize the mutation window, its upper and lower bounds must be defined. The lower bound of the window (denoted U_*) corresponds to the mutation rate at which the rescue probability rises to $1/2$. Thus, this lower bound is only defined if the height of the window lies above or at $1/2$ ($\max(P_R) \geq 1/2$). The upper bound is set to the mutation rate U_{max} beyond which certain extinction is enforced by lethal mutagenesis. The ER probability drops off

very sharply close to U_{max}, so that, approximatively, ER is only likely within the mutation window $U_* \leq U \leq U_{max}$. These two bounds are derived in Appendix I Eq. (A17):

$$U_{max} = \frac{4\, r_{max}^2}{n^2 \lambda}$$
$$U_* \approx \frac{1}{\lambda}\left(\frac{2\, g(y_D)\, r_{\max}}{\mathcal{W}(5.3\, g(y_D)\, N_0^2 r_{\max}^2)}\right)^2 \underset{N_0 \to \infty}{\approx} \frac{4\, g(y_D)^2\, r_{\max}^2}{\lambda \log\left(\frac{N_0^2}{\log(N_0^2)}\right)^2} \qquad [7]$$

where $\mathcal{W}(.)$ is the Lambert *W* function, which converges to $\mathcal{W}(z) \approx \log(z/\log(z))$ as z gets large (yielding the right hand side approximation above). Here, $g(y_D)$ is the function of stress intensity given in Eq.[6], which describes how stress intensity ($y_D = r_D/r_{max}$) affects ER rates. Depending on the scenario, one uses $g(y_D) = g_{DN+SV}(y_D)$ or $g(y_D) = g_{DN}(y_D)$ in the presence or absence of standing variance, respectively (note that the window is always wider in the latter case).

Figure 4 illustrates, for an initially clonal population, the sharpness of the transition from ER being almost certain to being highly unlikely ($P_R = 1$ to $P_R = 0$) as a function of U and r_D. It also shows the accuracy of the approximation for U_* in Eq.[7] (dashed black line), compared to its numerical estimation from Eq.[5] (color gradient). **Supplementary Figure 5** shows a similar result for a population starting with standing genetic variance.

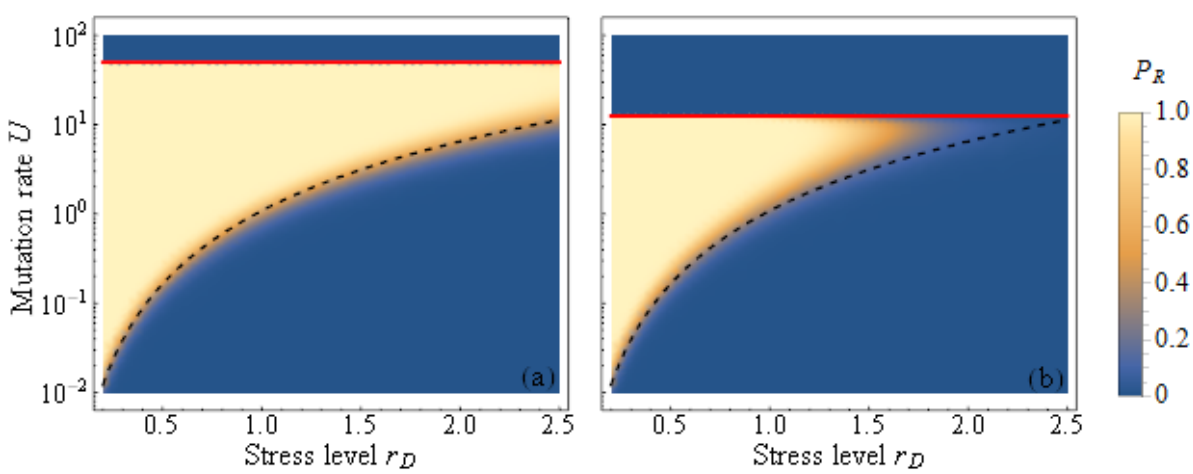

455 ***Figure 4:*** *ER probabilities from de novo mutants only (Eq.[5]) for different values of r_D and U. The*
456 *color gradient gives the value of P_R (see legend). The red straight line corresponds to $U = U_{max}$*
457 *(Eq.[7]) and the black dashed line corresponds to $U = U_*$ $(P_R = 1/2)$ (Eq.[7]). For a given U, the*
458 *ER probability drops sharply from $P_R = 1$ (light yellow) to $P_R = 0$ (blue), over a short increase in r_D.*
459 *For a given r_D, P_R rises sharply as U increases about U_* and then drops sharply as U increases*
460 *around U_{max}. Other parameters are $r_{max} = 1$, $N_0 = 10^4$ and $\lambda = 5.10^{-3}$. $n = 4$ in panel (a) and*
461 *$n = 8$ in panel (b).*

462

463 The upper bound U_{max} is independent of initial conditions or stochasticity, as lethal
464 mutagenesis depends on the deterministic equilibrium state of the population, once adapted to
465 the stress. Therefore, U_{max} does not depend on the presence or absence of initial standing
466 variance, the decay rate imposed by the environmental change (y_D) or the initial population
467 size N_0. On the contrary, the lower bound U_* depends on these factors as it is determined by the
468 capacity of the population to transiently adapt to the new conditions. It shows, however, little
469 dependence on dimensionality (n), as is also apparent in **Figure 4**, by the accuracy of Eq.[7], which
470 is independent of n. Overall, the width of the mutation window where ER is likely decreases with
471 increasing stress r_D (**Figure 4**) and increases with initial population size N_0 (eq. [7]: U_* increases
472 with N_0, and U_{max} is unchanged). It decreases with dimensionality n and increases with the
473 maximum fitness in the new environment r_{max}, but only because the upper bound of the window,
474 U_{max} (eq. [7]), decreases with these parameters.

475 Finally, note that we focused on the effect of variation in U here, but similar results could be
476 obtained if λ was varied (as both parameters affect P_R as a product $\mu = \sqrt{U\,\lambda}$). This is apparent in
477 Eq.[7] where U and λ could be exchanged.

478

479 *Height of the window and "Mutation proof extinction":* within the mutation window ($U_* \leq U \leq$
480 U_{max}), the ER probability P_R rises above 50% and then drops back to zero. Yet, for more extreme
481 stresses, it cannot even reach above 50% for any value of the mutation rate: the height of the
482 mutation window lies below $1/2$). When this height is low, extinction is 'mutation proof', in that it
483 is highly likely whatever the mutation rate(s) U or the variance of mutational effects λ in the
484 population. To illustrate this, we compute the maximum of the ER probability $\max(P_R)$ when U

485 varies from U_c to U_{max}, by numerically evaluating Eq.[5] over this range. **Supplementary Figure 6**
486 shows detailed profiles of ER probabilities against mutation rates (illustrating how $\max(P_R)$ is
487 found), in the presence or absence of initial standing variance. **Figure 5** shows the maximum P_R
488 attainable as a function of r_D and N_0: it drops (transition from yellow to blue areas) with increasing
489 stress r_D and decreasing population size N_0. In this example, a large part of the combinations of
490 the two parameters N_0 and r_D correspond to $\max(P_R)$ lower than 10% (blue area below the lower
491 white dashed line in **Figure 5**). Therefore, for a given inoculum size N_0, there is always a threshold
492 of stress level beyond which ER is nearly impossible, whatever the mutation rates in the population.

493 A closed form approximation can be obtained to describe this transition (detailed in
494 Appendix I section VII): denote $r_D^*(p)$ the value of r_D at which $\max(P_R) = p$ for some $p \in [0,1]$.
495 We obtain the following simple expression for the threshold of level of stress beyond
496 which $\max(P_R)$ cannot exceed some level p, independently of μ:

$$r_D^*(p) = \frac{r_{max}}{n\,\delta} \log\left(\frac{N_0\, r_{max}}{n \log(1/(1-p))}\right) \text{ with} \begin{cases} DN : \delta = 0.6 \\ DN + SV : \delta = 0.31 \end{cases}. \qquad [8]$$

497 Setting $p \ll 1$ in Eq.[8] thus provides the stress level beyond which ER is very unlikely, whatever
498 the mutation rate U or phenotypic variance λ. This means, in particular, that the evolution of
499 higher mutation rates (via hypermutator strains) or higher phenotypic variance (larger λ) would
500 not allow the population to avoid extinction, when confronted to this stress level. The validity of
501 the heuristic in Eq. [8] is illustrated in **Figure 5**, where we see that the dashed lines ($r_D^*(p)$ with $p =$
502 $\{0.1, 0.5, 0.9\}$ see legend) accurately predict the transition from high to low values of $\max(P_R)$,
503 computed numerically from Eq.[5].

504 This whole argument applies to both DN and $DN + SV$ scenarios (by choosing δ
505 accordingly in Eq. [8]). Interestingly, we can also see that populations initially at mutation-selection
506 balance (standing genetic variation) can withstand stresses twice larger or maximal growth rates
507 twice smaller than populations only adapting from *de novo* mutations (initially clonal).

508

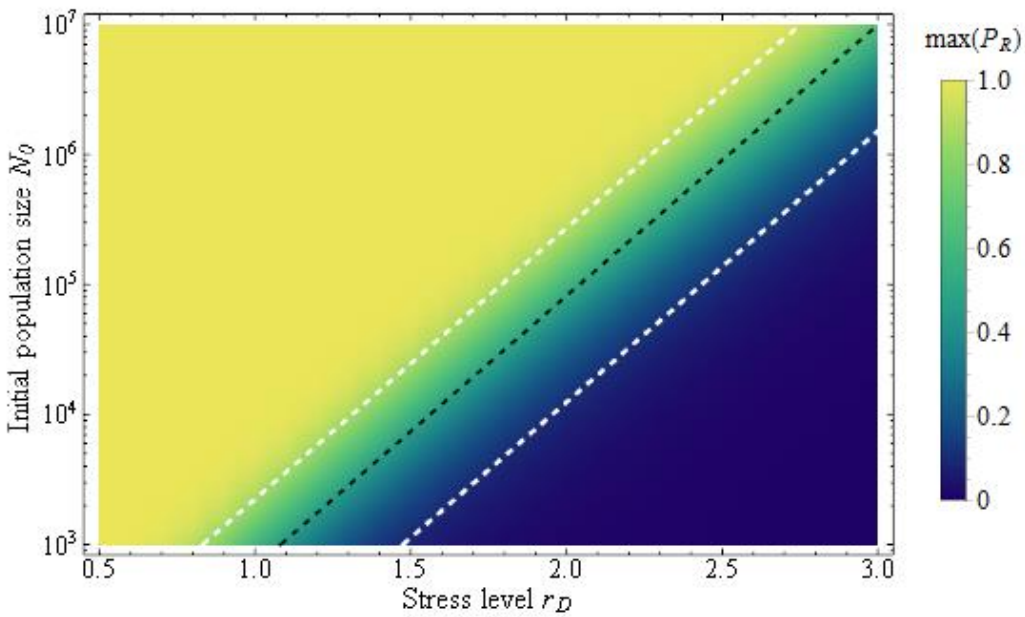

Figure 5: *Maximum ER probability reached as U is varied, for different values of r_D and N_0 for a population with no initial polymorphism.* The color gradient gives the value of $max(P_R)$ this time (see legend). *The black dashed line gives the value of $r_D^*(0.5)$ (Eq.[8]) and the white dashed lines the value of $r_D^*(0.1)$ and $r_D^*(0.9)$. The maximum of the ER probability attainable (for all possible U) drops sharply over a short range of increasing r_D for a given N_0, or over a short range of decreasing N_0 for a given r_D. Other parameters are $r_{max} = 0.5$, $n = 4$, and $\lambda = 5.10^{-3}$.*

Distribution of extinction times: From Eq.[4] we can derive the probability density $\varphi(t)$ of this distribution, in either of the two scenarios considered (purely clonal population DN or population at mutation-selection balance $DN + SV$). We get:

$$\varphi(t) = \frac{\partial_t P_{ext}(t)}{P_{ext}(\infty)} = 2\, N_0\, \frac{P_{ext}(t)}{P_{ext}(\infty)}\, \frac{\Psi'(t)}{\Psi(t)^2} \quad , \qquad [9]$$
$$\Psi(t) = \int_0^t h(\mu\, v)^{n/2}\, e^{-\frac{n}{2\epsilon} f(\mu\, v)}\, dv$$

where the functions $f(.)$ and $h(.)$ depend on the scenario considered and is given explicitly in Eq.[5]. **Figure 6** illustrates the accuracy of this result and how the distribution of extinction times

varies with stress intensity r_D and mutation rate U. In spite of neglecting evolutionary stochasticity, Eq.[9] still captures the shape and scale of extinction time distributions, in the WSSM regime.

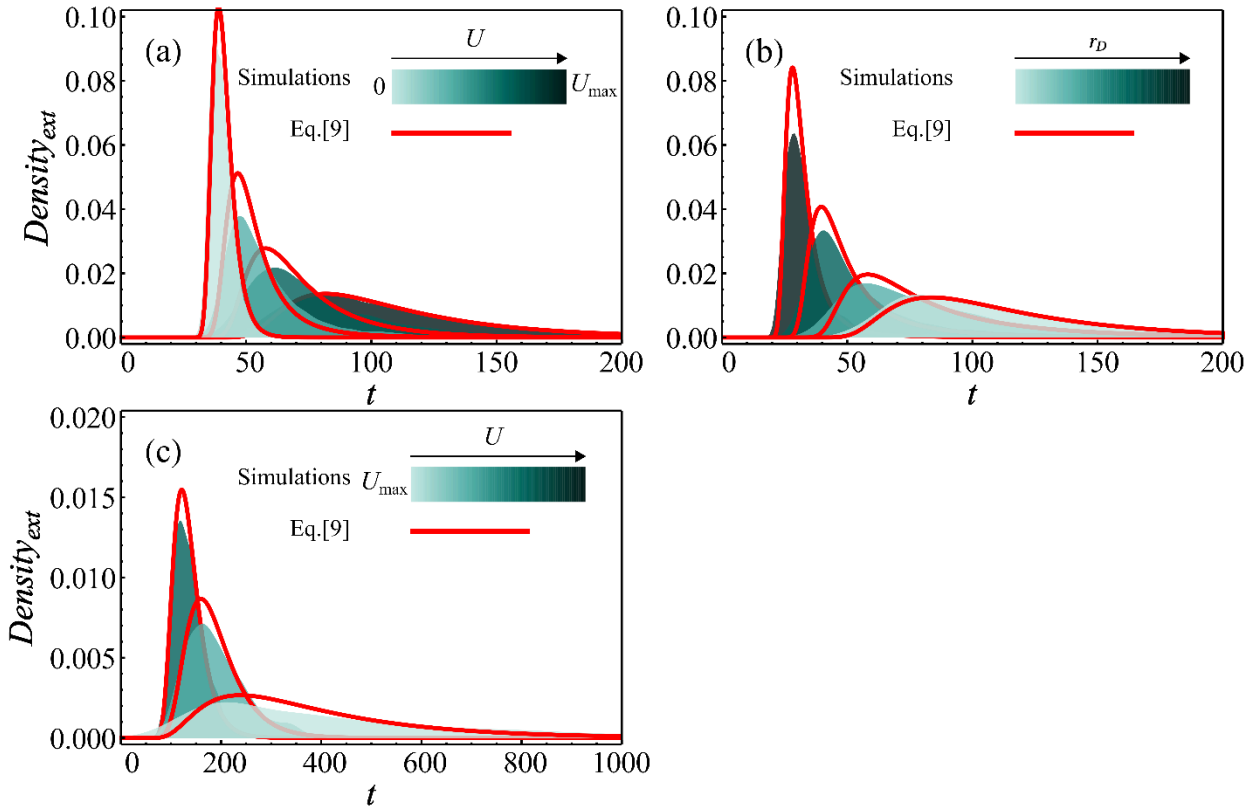

Figure 6: *Density of the extinction probability dynamics for different values of U (panel (a) and (c)) and r_D (panel (b)). The distributions of extinction times from simulations started with an isogenic population are shown by shaded histograms, with the corresponding theory (Eq.[9]) given by the plain red lines. The color gradient corresponds to increasing levels of r_D (panel (b)) or of U (lower range in panel (a) and higher range in panel (c), as indicated on the legend). Each simulated distributions is drawn from 1000 extinct populations among a varying number of replicates depending on the ER probability. The mutation rates covered in panel (a) are $U = \{0;\ 4\,U_c; 8\,U_c; 14\,U_c\}$ and in panel (c) are $U = \{2\,U_{max};\ 1.5\,U_{max};\ 1.1\,U_{max}\}$ and in both panel the decay rate is $r_D = 0.28$. The decay rate covered in panel (b) are $\{0.285; 0.33; 0.4; 0.5\}$ and the mutation rate is $U = 15\,U_c$. Other parameters are $N_0 = 10^5$, $n = 4$, $r_{max} = 0.1$ and $\lambda = 5.10^{-3}$.*

Figure 6b shows that decreasing the stress level (r_D) increases the mean persistence time of the population and also increases the variance of this duration. This behavior could be seen as a mere scaling: even in the absence of evolution the population takes longer time to get extinct with a smaller r_D. On the contrary, increasing the mutation rate, keeping it below the lethal

540 mutagenesis threshold ($0 \leq U \leq U_{max}$, **Figure 6a**), increases the mean and the variance of the
541 persistence time. This likely stems from subcritical mutations ($0 > r > r_D$, beneficial but not
542 resistant) that can transiently invade the population, thus delaying its extinction. However, beyond
543 the lethal mutagenesis threshold ($U > U_{max}$, **Figure 6c**), the trend is reversed: extinctions (which
544 are always certain then) occur faster at high mutation rates (panel c). Therefore, even in those
545 cases where ER probabilities are uninformative ($P_R = 0$), the distribution of extinction times
546 conveys important information on the underlying adaptive or maladaptive dynamics.

547

548 ## Discussion

549 We investigated the effect of an abrupt environmental change on the persistence of
550 asexual populations with a large mutational input of genetic variance (WSSM regime), adapting
551 either from *de novo* mutations arising after the environmental change (DN scenario) or from both
552 *de novo* and pre-existing mutations ($DN + SV$ scenario). In a previous study (Anciaux et al. 2018),
553 we studied evolutionary rescue when considering adaptation over a phenotype-fitness landscape
554 (FGM), which implies pervasive epistasis between multiple mutations and imposes a relationship
555 between the initial decay rate of the population, the proportion and growth rate of resistance
556 alleles, and their selective cost in the ancestral (before the stress) environment. However, we
557 assumed that rescue resulted from rare mutations with strong effects (SSWM). The key
558 contributions of the present model, building on our previous work, are to (i) allow for the
559 cumulative effect of multiple mutations and (ii) provide insights into the distribution of extinction
560 times in the presence of an evolutionary response.

561

562 **Single step (SSWM regime) *vs.* multiple step (WSSM) regimes in ER:** In spite of its complexity, the ER
563 process in high mutation rate regimes can readily be captured by simple analytic approximations
564 (Eqs.[5] and [6]), which neglect evolutionary stochasticity and only account for demographic
565 stochasticity. Overall, the SSWM and WSSM approximations roughly capture complementary
566 domains of the mutation rate spectrum (**Figures 1-3**).

567 This approach shows how multiple mutations allow withstanding higher stress than what
568 the single step approximation (SSWM in Anciaux *et al.* 2018) predicts (**Figures 1 and 3**). However,
569 this is only true for intermediate mutation rates: a further increase in mutation rate ultimately
570 shifts the system to a lethal mutagenesis regime (**Figures 2 to 4**). Indeed, the dependence between
571 the ER probability and the mutation rate is not monotonic. The model shows an optimal mutation
572 rate for the ER probability, at which the maximal ER probability may be less than 1 (depending on
573 the stress, **Figure 5**). Beyond this rate, the ER probability drops down, to some point (U_{max}, Eq. **[7]**)
574 where the mutation load is so large that absolute fitness is negative at mutation selection balance.
575 This non-monotonic dependence reflects the continuum between ER and lethal mutagenesis along
576 a gradient of mutation rates.

577 The strategy used here (Eq. [4]) to cope with multiple mutations could in principle be
578 applied to many different models: in fact to any for which deterministic mean fitness trajectories
579 are known (equivalent to eqs. [2] or [3]). In particular, it could be used to extend the two broad
580 classes of ER models defined in (Alexander et al. 2014). First, the 'origin-fixation' models, which
581 consider single step rescue with stochastic demography (e.g. Orr and Unckless 2008, 2014), could
582 be extended to multiple step rescue, as was done for (Anciaux et al. 2018) in the case of the FGM.
583 Second, the 'quantitative genetics' models of ER, which consider deterministic evolution and
584 demography, could be extended to account for stochastic demography. As these models are also
585 obtained in the same limit of weak selection strong mutation (and loose linkage between loci) they
586 should a priori be easy to handle with the approximation in Eq. [4]. The $DN + SV$ scenario here,
587 shares strikingly similar properties (in its phenotypic evolution part) with models of sexual
588 evolution that assume a constant genetic variance for traits (also maintained by recombination in
589 the latter model, not only by mutation). We conjecture that our results would easily extend to this
590 context.

591

592 **Comparison to existing ER models:** Some of our key previous findings (Anciaux et al. 2018),
593 regarding how ER depends on the parameters of the fitness landscape (FGM here) are still valid in
594 the more polymorphic WSSM regime. The main common features are (i) the sharp decrease of ER

probabilities with stress (decay rate r_D), (ii) their log-linear increase with initial population size N_0, (iii) the fact that standing variance allows to withstand higher stress, (vi) the limited effect of dimensionality n (eq. [6]). The effect of initial population size ($P_R = 1 - e^{-N_0\,\omega}$ eq.[5]) is exactly the same as in previous models where ER stemmed from single mutants (SSWM regime Orr and Unckless 2008, 2014; Martin *et al.* 2013; Anciaux *et al.* 2018). This is expected of any model ignoring evolutionary and demographic interactions between individuals: each of the N_0 lineages initially present contributes independently to ER (with some rate ω per individual). Decay rate has a broadly similar (but quantitatively different) effect in previous ER models not based on a fitness landscape. The other parameters (r_{max}, n, λ) are not defined outside the FGM. More generally, the key implications of considering the FGM to model ER are detailed more thoroughly in Anciaux *et al.* (2018).

Experimental test and parametrization: To experimentally test the prediction, the assumptions of the WSSM regime *a priori* imply to use organisms with relatively high mutation rates, such as viruses, highly mutating strains of bacteria or possibly cancer cells. Empirically mutation effects and rates, at least in microbes, are typically scaled by growth rates. In our model, these scaled parameters are $\bar{s} \equiv n\,\lambda/(2\,r_{max})$ and $u \equiv U/r_{max}$. If r_{max} is approximately equal to a birth rate (i.e. optimal genotype have a small death rate) $\bar{s}$ is akin to a mean mutation effect per division, while u is akin to a mutation rate per division. Expressed in these parameters, the WSSM approximation (Eq.[5]) applies when $u_c \equiv n/2\,\bar{s}\,r_{max} \ll u$, lethal mutagenesis occurs when $u = u_{max} \equiv 2/(n\,\bar{s})$ and the intermediate mutation weak selection approximation (Eq.[6]) is valid when $u_c \ll u \ll 1$.

For a complete experimental test of the predictions, the parameters N_0, U, r_D, r_{max}, λ and n must be measured. The methods and challenges in estimating these parameters are discussed in Anciaux *et al.* 2018). Note however that (i) the results only depend on the product $\mu = \sqrt{U\,\lambda}$ and that (ii) an error on the dimensionality may not be critical given its relatively small effect. Furthermore, if the model is valid, fitting an observed distribution of extinction times (**Figure 6**) might provide estimates of most parameters of the model. This would allow using not only the

623 information from rescued populations but that from extinct ones. Such empirical test would
624 require fine-scale time series of the population size or at least the extinction status over time.

625

626

627 **Treatment against pathogens, hyper-mutators and lethal mutagenesis:** Our model as well as
628 previous ones all suggest that the effectiveness of a given treatment depends on the mutation rate
629 of the organism. Polymorphism for mutation rate and invasion of hyper-mutator genotypes are
630 thus potentially important issues for treatments against pathogens. However, our results suggest
631 that a sufficiently strong stress could be effective in spite of hyper-mutator evolution. Indeed,
632 because of the lethal mutagenesis effect (**Figure 2**), ER is only possible within a mutation rate
633 window: a hyper-mutator would have to hit this window to be advantageous, and the width of the
634 window narrows with increased stress (**Figure 4**). At sufficiently higher stress levels, ER is unlikely
635 whatever the mutation rate (**Figure 5**), making these strong treatments robust to hyper-mutator
636 evolution. Whether this pattern is confirmed empirically and whether the required treatment
637 levels are then not too harmful for the treated subject remain open questions. Note also that the
638 same line of argument could be used, not for mutation rate evolution, but for the evolution of
639 phenotypic variance, as the end result depends on the product $\mu^2 = U\,\lambda$.

640 Our model covers the continuum from stress induced extinction to extinction induced by
641 lethal mutagenesis. The latter might be an option, especially for organisms for which no "stress
642 treatment" exists, or whose high mutation rates (above U_* in our model) allows them to withstand
643 even strong stresses. Our results indeed confirm that increasing the mutation rate in this context
644 (above U_{max}) will allow to fully eliminate the population. The addition of a stressor might also help
645 in the process, as has been suggested before (Pariente et al. 2001, 2003, 2005): indeed, the ER
646 probability does drop faster with increasing U (as we approach U_{max}) in the presence of a strong
647 stress (with high y_D), see **Supplementary Figure 6**.

648

649 **Treatment duration issues**: One may also wonder how long a treatment must last (be it by stress
650 effect or by lethal mutagenesis) for it to be efficient. From the distribution of extinction times
651 (**Figure 6**), it is possible to predict the duration of the treatment needed to get rid of, say, 99% of
652 the pathogen populations. Strong stresses (dark blue histogram in **Figure 6b**) tend to both decrease
653 the overall ER probability and shrink the distribution of times to extinction. This means they are
654 more efficient overall and require shorter treatment durations, with less risk associated with
655 imperfect treatment compliance. However, when the mutation rate increases towards U_{max}
656 (treatment by lethal mutagenesis), although extinction becomes highly likely ($P_R \to 0$, **Figure 2**),
657 extinction times get more variable and the mode of the distribution is higher (**Figure 6a**). If the
658 mutation rate increases beyond U_{max}, the opposite pattern is observed: the distribution of
659 extinction times shrinks as U increases further away from U_{max} (**Figure 6c**). Hence, a treatment by
660 lethal mutagenesis, even if guaranteeing total extinction after infinite time, may need to be applied
661 for a long time to significantly decrease ER probability (if the resulting U is close to U_{max}). Thus,
662 observed distributions of extinction times hold valuable information.

663

664 **Limits of the model:** Obviously, the different results and applications described above are limited
665 by the hypotheses of the model. First, the model ignores density or frequency-dependent effects.
666 Moreover, the approximation of the demographic dynamics by a Feller diffusion imposes that
667 demographic variations remain smooth, which may be inaccurate, e.g. for some viruses showing
668 occasional large burst events. The Feller diffusion can also fail to predict discrete time demography
669 (used here in the simulations) at high growth rates per generation ($r \geq 1$). This could be overcome
670 by using a numerical analysis of discrete time inhomogeneous branching processes instead of the
671 Feller diffusion. Second, the model assumes a WSSM regime, which excludes its application to
672 organisms with lower mutation rates (relative to selection intensity $U < U_c$). This could however
673 be handled by complementary models under the SSWM regime such as (Anciaux et al. 2018), under
674 the same landscape assumptions. Finally, our results assume a sharp change in the environment,
675 which does not reflect all forms of stresses, including in the context of sudden treatment (e.g.
676 antibiotics can have complex pharmacokinetic patterns over time Regoes et al. 2004). In that

677 respect, extensions to more complex ecological scenarios might be useful: some are *a priori*
678 possible using the same broad modelling framework as used here.

679

680 Bibliography

681

682 Alexander, H. K., G. Martin, O. Y. Martin, and S. Bonhoeffer. 2014. Evolutionary rescue: linking theory for
683 conservation and medicine. Evol. Appl. 7:1161–1179.

684 Anciaux, Y., L.-M. Chevin, O. Ronce, and G. Martin. 2018. Evolutionary Rescue over a Fitness Landscape.
685 Genetics 209:265–279.

686 Arias, A., L. Thorne, and I. Goodfellow. 2014. Favipiravir elicits antiviral mutagenesis during virus
687 replication in vivo. eLife 3.

688 Bank, C., N. Renzette, P. Liu, S. Matuszewski, H. Shim, M. Foll, D. N. A. Bolon, K. B. Zeldovich, T. F. Kowalik,
689 R. W. Finberg, J. P. Wang, and J. D. Jensen. 2016. An experimental evaluation of drug-induced
690 mutational meltdown as an antiviral treatment strategy. Evolution 70:2470–2484.

691 Bansaye, V., and F. Simatos. 2015. On the scaling limits of Galton-Watson processes in varying
692 environments. Electron. J. Probab. 20.

693 Bell, G. 2017. Evolutionary Rescue. Annu. Rev. Ecol. Evol. Syst. 48:605–627.

694 Bull, J. J., R. Sanjuán, and C. O. Wilke. 2007. Theory of Lethal Mutagenesis for Viruses. J. Virol. 81:2930–
695 2939.

696 Bull, J. J., and C. O. Wilke. 2008. Lethal Mutagenesis of Bacteria. Genetics 180:1061–1070.

697 Bürger, R., and C. Krall. 2004. Quantitative-genetic models and changing environments.

698 Carlson, S. M., C. J. Cunningham, and P. A. H. Westley. 2014. Evolutionary rescue in a changing world.
699 Trends Ecol. Evol. 29:521–530.

700 Couce, A., A. Rodríguez-Rojas, and J. Blázquez. 2015. Bypass of genetic constraints during mutator
701 evolution to antibiotic resistance. Proc R Soc B 282:20142698.

702 Eliopoulos, G. M., and J. Blázquez. 2003. Hypermutation as a Factor Contributing to the Acquisition of
703 Antimicrobial Resistance. Clin. Infect. Dis. 37:1201–1209.

704 Feder, A. F., S.-Y. Rhee, S. P. Holmes, R. W. Shafer, D. A. Petrov, and P. S. Pennings. 2016. More effective
705 drugs lead to harder selective sweeps in the evolution of drug resistance in HIV-1. Elife 5:e10670.

706 Feller, W. 1951. Diffusion processes in genetics. University of California Press Berkeley, Calif.

Fisher, R. A. 1930. The Genetical Theory of Natural Selection. Oxford University Press.

Gerrish, P. J., and R. E. Lenski. 1998. The fate of competing beneficial mutations in an asexual population. Genetica 102:127.

Gomulkiewicz, R., and R. D. Holt. 1995. When does Evolution by Natural Selection Prevent Extinction? Evolution 49:201.

Gomulkiewicz, R., R. D. Holt, M. Barfield, and S. L. Nuismer. 2010. Genetics, adaptation, and invasion in harsh environments. Evol. Appl. 3:97–108.

Gomulkiewicz, R., S. M. Krone, and C. H. Remien. 2017. Evolution and the duration of a doomed population. Evol. Appl. n/a-n/a.

Gonzalez, A., O. Ronce, R. Ferriere, and M. E. Hochberg. 2013. Evolutionary rescue: an emerging focus at the intersection between ecology and evolution. Philos. Trans. R. Soc. B Biol. Sci. 368:20120404–20120404.

Greenspoon, P. B., and N. Mideo. 2017. Evolutionary rescue of a parasite population by mutation rate evolution. Theor. Popul. Biol. 117:64–75.

Holt, R., M. Barfield, and R. Gomulkiewicz. 2004. Temporal Variation Can Facilitate Niche Evolution in Harsh Sink Environments. Am. Nat. 164:187–200.

Holt, R. D., R. Gomulkiewicz, and M. Barfield. 2003. The phenomenology of niche evolution via quantitative traits in a “black-hole” sink. Proc. R. Soc. B Biol. Sci. 270:215–224.

Kreiner, J. M., J. R. Stinchcombe, and S. I. Wright. 2018. Population Genomics of Herbicide Resistance: Adaptation via Evolutionary Rescue. Annu. Rev. Plant Biol. 69:611–635.

Lande, R. 1976. Natural Selection and Random Genetic Drift in Phenotypic Evolution. Evolution 30:314.

Lande, R. 1980. The Genetic Covariance Between Characters Maintained by Pleiotropic Mutations. Genetics 94:203–215.

Liu, L. L., F. Li, W. Pao, and F. Michor. 2015. Dose-Dependent Mutation Rates Determine Optimum Erlotinib Dosing Strategies for EGFR Mutant Non-Small Cell Lung Cancer Patients. PLoS ONE 10.

Loeb, L. A. 2001. A Mutator Phenotype in Cancer. Cancer Res. 61:3230–3239.

Loeb, L. A., J. M. Essigmann, F. Kazazi, J. Zhang, K. D. Rose, and J. I. Mullins. 1999. Lethal mutagenesis of HIV with mutagenic nucleoside analogs. Proc. Natl. Acad. Sci. 96:1492–1497.

Martin, G., R. Aguilée, J. Ramsayer, O. Kaltz, and O. Ronce. 2013. The probability of evolutionary rescue: towards a quantitative comparison between theory and evolution experiments. Phil Trans R Soc B 368:20120088.

Martin, G., and S. Gandon. 2010. Lethal mutagenesis and evolutionary epidemiology. Philos. Trans. R. Soc. Lond. B Biol. Sci. 365:1953–1963.

740 Martin, G., and L. Roques. 2016. The Non-stationary Dynamics of Fitness Distributions: Asexual Model with
741 Epistasis and Standing Variation. Genetics genetics.116.187385.

742 Matuszewski, S., L. Ormond, C. Bank, and J. D. Jensen. 2017. Two sides of the same coin: A population
743 genetics perspective on lethal mutagenesis and mutational meltdown. Virus Evol. 3.

744 McCandlish, D. M., and A. Stoltzfus. 2014. Modeling Evolution Using the Probability of Fixation: History
745 and Implications. Q. Rev. Biol. 89:225–252.

746 Orr, H. A., and R. L. Unckless. 2008. Population Extinction and the Genetics of Adaptation. Am. Nat.
747 172:160–169.

748 Orr, H. A., and R. L. Unckless. 2014. The Population Genetics of Evolutionary Rescue. PLOS Genet.
749 10:e1004551.

750 Pariente, N., A. Airaksinen, and E. Domingo. 2003. Mutagenesis versus Inhibition in the Efficiency of
751 Extinction of Foot-and-Mouth Disease Virus. J. Virol. 77:7131–7138.

752 Pariente, N., S. Sierra, and A. Airaksinen. 2005. Action of mutagenic agents and antiviral inhibitors on foot-
753 and-mouth disease virus. Virus Res. 107:183–193.

754 Pariente, N., S. Sierra, P. R. Lowenstein, and E. Domingo. 2001. Efficient Virus Extinction by Combinations
755 of a Mutagen and Antiviral Inhibitors. J. Virol. 75:9723–9730.

756 Ramsayer, J., O. Kaltz, and M. E. Hochberg. 2013. Evolutionary rescue in populations of Pseudomonas
757 fluorescens across an antibiotic gradient. Evol. Appl. 6:608–616.

758 Regoes, R. R., C. Wiuff, R. M. Zappala, K. N. Garner, F. Baquero, and B. R. Levin. 2004. Pharmacodynamic
759 Functions: a Multiparameter Approach to the Design of Antibiotic Treatment Regimens.
760 Antimicrob. Agents Chemother. 48:3670–3676.

761 Springman, R., T. Keller, I. J. Molineux, and J. J. Bull. 2010. Evolution at a High Imposed Mutation Rate:
762 Adaptation Obscures the Load in Phage T7. Genetics 184:221–232.

763 Taddei, F., M. Radman, J. Maynard-Smith, B. Toupance, P. H. Gouyon, and B. Godelle. 1997. Role of
764 mutator alleles in adaptive evolution. Nature 387:700–702.

765 Tenaillon, O. 2014. The Utility of Fisher's Geometric Model in Evolutionary Genetics. Annu. Rev. Ecol. Evol.
766 Syst. 45:179–201.

767 Uecker, H. 2017. Evolutionary rescue in randomly mating, selfing, and clonal populations. Evolution
768 71:845–858.

769 Uecker, H., and J. Hermisson. 2016. The Role of Recombination in Evolutionary Rescue. Genetics 202:721–
770 732.

771 Wilson, B. A., P. S. Pennings, and D. A. Petrov. 2017. Soft Selective Sweeps in Evolutionary Rescue.
772 Genetics 205:1573–1586.

773 Wylie, C. S., and E. I. Shakhnovich. 2012. Mutation Induced Extinction in Finite Populations: Lethal
774 Mutagenesis and Lethal Isolation. PLOS Comput. Biol. 8:e1002609.

775